

Published in final edited form as:

Sci Signal. ; 1(43): ra11. doi:10.1126/scisignal.1159665.

Essential Role of DAP12 Signaling in Macrophage Programming into a Fusion-Competent State

Laura Helming^{1,*}, Elena Tomasello^{2,3,4}, Themis R. Kyriakides^{5,6,7}, Fernando O. Martinez¹, Toshiyuki Takai^{8,9}, Siamon Gordon^{1,†,‡}, and Eric Vivier^{2,3,4,10,†,‡}

¹Sir William Dunn School of Pathology, University of Oxford, South Parks Road, Oxford OX1 3RE, UK.

²Centre d'Immunologie de Marseille-Luminy, Université de la Méditerranée, case 906, Campus de Luminy, 13288 Marseille, France.

³INSERM, U631, case 906, Campus de Luminy, 13288 Marseille, France.

⁴CNRS, UMR6102, case 906, Campus de Luminy, 13288 Marseille, France.

⁵Vascular Biology and Therapeutics Program, Boyer Center for Molecular Medicine, Yale University School of Medicine, New Haven, CT 06520, USA.

⁶Department of Pathology, Yale University School of Medicine, New Haven, CT 06520, USA.

⁷Department of Biomedical Engineering, Yale University School of Medicine, New Haven, CT 06520, USA.

⁸Department of Experimental Immunology, Institute of Development, Aging and Cancer, Tohoku University, Seiryō 4-1, Aoba-ku, Sendai 980-8575, Japan

⁹Core Research for Evolutional Science and Technology (CREST), Japan Science and Technology Corporation (JST), Honcho 4-1-8, Kawaguchi, Saitama 332-0012, Japan.

¹⁰Assistance Publique-Hôpitaux de Marseille, Hôpital de la Conception, 13385 Marseille, France.

Abstract

Multinucleated giant cells, formed by fusion of macrophages, are a hallmark of granulomatous inflammation. With a genetic approach, we show that signaling through the adaptor protein DAP12 (DNAX activating protein of 12 kD), its associated receptor triggering receptor expressed by myeloid cells 2 (TREM-2), and the downstream protein tyrosine kinase Syk is required for the cytokine-induced formation of giant cells and that overexpression of DAP12 potentiates macrophage fusion. We also present evidence that DAP12 is a general macrophage fusion regulator and is involved in modulating the expression of several macrophage-associated genes, including those encoding known mediators of macrophage fusion, such as *DC-STAMP* and *Cadherin 1*. Thus, DAP12 is involved in programming of macrophages through the regulation of gene and protein expression to induce a fusion-competent state.

INTRODUCTION

Multinucleated giant cells were first described by Langhans in 1868 and are consistently present in tuberculoïd granulomas (1). Multinucleated giant cells are not only characteristic of

†To whom correspondence should be addressed. E-mail: E-mail: siamon.gordon@path.ox.ac.uk (S.G.) and E-mail: vivier@ciml.univ-mrs.fr (E.V.).

*Present address: Institute of Medical Microbiology, Immunology and Hygiene, Technical University of Munich, Trogerstrasse 30, 81675 Munich, Germany.

‡Joint senior authors.

tuberculosis, but also are a constituent feature in granulomatous conditions, including sarcoidosis and the parasitic infection schistosomiasis as well as the foreign body reaction, which is the host response to large implanted biomaterials (2,3). Multinucleated giant cells originate from fusion of macrophages that are recruited to the site of granulomatous inflammation (4). Cell–cell fusion is a characteristic feature of multicellular organisms and, in mammals, cell fusion is indispensable for fertilization and skeletal muscle and trophoblast formation (5,6). Although sperm–egg, myoblast, and trophoblast fusion are linked to obvious functions, the functional consequences of granuloma-associated giant cell formation remain enigmatic (3). Giant cells associated with implanted materials (foreign body giant cells) may display an enhanced capacity to degrade large particles (7) and, therefore, could be deleterious for implants. Tuberculosis-associated giant cells have been associated with restriction of cell-to-cell spread of mycobacteria (8) and with increased metalloproteinase secretion (9), which may potentially contribute to tissue destruction. Thus, it is not clear if the formation of giant cells during granulomatous inflammation is beneficial or detrimental for the infected individual. Fusion of macrophages also leads to the formation of osteoclasts, the cells that ensure lifelong renewal of the skeleton (10). Although giant cells and osteoclasts are both formed by macrophage fusion, it remains to be elucidated if they share a similar mechanism of fusion and if they exhibit an analogous function. Whereas osteoclast formation is stimulated by receptor activator of nuclear factor kappa B ligand (RANKL) and the growth factor macrophage colony-stimulating factor (M-CSF), the stimuli inducing the formation of giant cells *in vivo* are less well defined but may involve the cytokines present in granulomas, particularly the cytokine interleukin 4 (IL-4) (3). Detailed knowledge of the mechanism of giant cell formation may lead to a better understanding of their function during granulomatous diseases. Previously, we established an *in vitro* assay for studying the mechanism of IL-4–induced giant cell formation (11), which may aid in this investigation.

The signaling adaptor protein DAP12 [(DNAX activating protein of 12 kD), also known as KARAP (killer cell activating receptor-associated protein) or TYROBP (tyrosine kinase binding protein)] was originally identified and characterized in natural killer (NK) cells (12–14) and is known to play a role in macrophage fusion during osteoclast formation (15,16). Whether DAP12 is also involved in macrophage fusion leading to giant cell formation is unknown. DAP12 is a transmembrane protein present at the cell surface as a disulfide-bonded homodimer and bears an immunoreceptor tyrosine-based activation motif (ITAM). DAP12 is present in hematopoietic cells and associates with various cell surface receptors in lymphoid and myeloid cells (17–19). Upon engagement of DAP12-associated receptors, the tyrosine residues in the DAP12 ITAM are phosphorylated, leading to the recruitment and activation of the protein tyrosine kinases Syk and ZAP70, which in turn lead to the activation of phosphatidylinositol 3-kinase (PI3K) (20). Several DAP12-associated receptors—triggering receptors expressed by myeloid cells (TREM)-1, 2, and 3; myeloid DAP12-associating lectin 1; CD200R-like proteins CD200R3 and R4; and CD300C, D, and E (19)—are present on macrophages. Based on the association of DAP12 with activating receptors in NK cells, studies on the function of DAP12 and its associated receptors in macrophages have mainly focused on its role in macrophage activation. In this capacity, the engagement of TREM-1 amplified signals of Toll-like receptors (TLRs) and other pattern recognition receptors (21), whereas activation of TREM-2, another DAP12-associated receptor, inhibited TLR responses (22,23). In addition to its role in macrophage activation by innate stimuli, DAP12 appears to be involved in integrin signaling in macrophages (24).

In humans, mutations of *DAP12* or *TREM-2* lead to polycystic lipomembranous osteodysplasia with sclerosing leukoencephalopathy (PLOS), which is associated with bone lesions and osteoporotic features (15,25). This phenotype is based on impaired osteoclast differentiation and function (15,25). DAP12-deficient mice have been generated either by partial gene deletion (16,26) or by mutation of the *DAP12* gene, leading to expression of a nonfunctional version

of the DAP12 protein (27). DAP12-deficient mice were found to exhibit defective bone resorption *in vivo* as well as impaired osteoclast differentiation and multinucleation *in vitro* (16,28,29). During osteoclast differentiation, DAP12 appears to act in concert with the Fc receptor common γ subunit (FcR γ) (30) and contributes to macrophage fusion during this process (29). In differentiated osteoclasts, DAP12 participates with Syk, c-Src, and the $\alpha\beta 3$ integrin to contribute to bone resorption (31).

There is evidence that DAP12 may not only be involved in osteoclast differentiation but also takes part in macrophage fusion leading to the formation of multinucleated giant cells. DAP12 gain-of-function transgenic mice, which display a fatal inflammatory syndrome, exhibit spontaneous formation of multinucleated giant cells in the lung in the apparent absence of pathogens (32). In this study, we utilized a genetic approach to dissect the role of the DAP12-dependent signaling pathway in the formation of multinucleated giant cells.

RESULTS

DAP12 deficiency results in impaired macrophage fusion

We asked if DAP12 is involved in the formation of multinucleated giant cells induced by IL-4. Using a bifluorescent macrophage fusion assay (11), we quantified IL-4-induced fusion in inflammatory macrophages recruited to the peritoneum after the injection of thioglycollate (thioglycollate-elicited peritoneal macrophages, ThioM Φ s) from DAP12-deficient mice. We used DAP12-KO macrophages, which do not express DAP12 protein (16), as well as macrophages from DAP12 loss-of-function mice (DAP12-KI), which express a mutant version of the DAP12 protein that is deficient in its signaling capacity because of mutation of the essential Y⁷⁵ residue in the ITAM motif (27). IL-4-induced macrophage fusion in DAP12-KO and DAP12-KI macrophages was reduced when compared to that of the wild-type (WT) control and was comparable to that of unstimulated controls (Fig. 1, A and B). To determine if DAP12 is required on all fusion partners combining to form a giant cell, CFSE (carboxyfluorescein succinimidyl ester, green)-labeled DAP12-KI macrophages were mixed with PKH26 (Paul Karl Horan 26, red)-labeled WT macrophages and incubated with IL-4. No colocalization and, therefore, no fusion of WT with DAP12-KI macrophages were observed (Fig. 1, A and B). Macrophage cultures were analyzed in greater detail by staining with Hemacolor. Macrophage fusion was not completely abolished in DAP12-KI and DAP12-KO macrophages and some multinucleated cells were formed after IL-4 stimulation (Fig. 1C); however, quantitation of macrophage fusion by counting the nuclei of single cells and giant cells showed that the degree of macrophage fusion was significantly reduced in DAP12-KO and DAP12-KI macrophages with and without IL-4 stimulation (Fig. 1D). This result was obtained with all IL-4 doses and incubation times tested (Fig. 1E). We conclude that DAP12 signaling is involved in macrophage fusion. Several DAP12-associated receptors depend on the presence of DAP12 for stable cell surface expression through association with DAP12 (17–19). Because fusion was deficient not only in DAP12-KO macrophages lacking the DAP12 protein but also in DAP12-KI macrophages deficient only in DAP12 ITAM signaling, we can conclude that DAP12 ITAM is involved in macrophage fusion. We concentrated on DAP12-KI macrophages for further analysis.

DAP12 deficiency does not affect macrophage maturation

It has been proposed that DAP12 is involved in myeloid differentiation (33). Deficient macrophage maturation in the absence of DAP12 signaling could potentially account for the defect in macrophage fusion. We, therefore, analyzed the percentage of F4/80⁺/CD11b⁺ macrophages in the spleen and the peritoneal cavity with and without injection of thioglycollate. Macrophage numbers were unaffected in DAP12-KI mice (Fig. 2A). The abundance of CD11b was also normal in DAP12-KI splenic, resident peritoneal, and thioglycollate-

elicited macrophages (table S1). In addition, analysis of the presence of macrophage markers in different tissues by immunohistochemistry showed that the macrophage markers CD68, EMR1 (F4/80), the mannose receptor, and MARCO were present with the expected distributions in spleen, gut, lung, and thymus of DAP12-KI mice (Fig. 2B, fig. S1). Thus, the absence of DAP12 signaling does not impair macrophage maturation.

Defective $\beta 2$ integrin signaling does not account for the fusion defect in DAP12 loss-of-function macrophages

In macrophages, DAP12 is involved in $\beta 2$ integrin activation (24), which could potentially influence macrophage fusion (34). One of the $\beta 2$ integrin-containing receptors present in macrophages is MAC1, which is composed of an alpha M subunit called CD11b and a beta 2 subunit called CD18. Macrophage adhesion to the fusogenic Permax surface used in our macrophage fusion assay is not mediated by $\beta 2$ integrins (11); thus, it is unlikely that defective $\beta 2$ activation is responsible for the fusion defects detected in the DAP12-KI and DAP12-KO cells. In addition, we analyzed macrophage fusion in ThioM Φ from MAC1 (CD11b/CD18)-deficient mice. Although a significant reduction in macrophage fusion could be observed in MAC1-KO macrophages (Fig. 3A), this defect was not as drastic as that observed for the DAP12-deficient cells (Fig. 1B). Furthermore, analysis of macrophage fusion in the presence of a CD18-blocking antibody produced only a slight reduction in macrophage fusion, which did not reach statistical significance (Fig. 3B). Control immunoglobulin G1 (IgG1) antibodies had no effect on macrophage fusion (Fig. 3C). Although $\beta 2$ integrins appear to play a minor role during macrophage fusion, deficient integrin activation cannot account for the drastic fusion defect seen in the absence of DAP12 signaling.

Targeted DAP12 knockdown leads to reduced IL-4-induced macrophage fusion

To confirm the requirement of DAP12 for maximal macrophage fusion but not adhesion or macrophage differentiation, we performed RNA silencing in *in vitro* differentiated bone marrow-derived macrophages (BMMs) after their adhesion to the fusogenic surface. Although ThioM Φ can fuse in response to stimulation with IL-4 alone (11), BMMs require a combination of IL-4 and GM-CSF (granulocyte-macrophage colony-stimulating factor) to induce giant cell formation (35). Targeted knockdown of DAP12 with the use of Stealth RNA interference (RNAi) significantly inhibited BMM fusion stimulated by combined exposure to IL-4 and GM-CSF (Fig. 4A). Furthermore, the requirement for DAP12 for the formation of multinucleated giant cells is not restricted to inflammatory ThioM Φ but extends to *in vitro* differentiated BMM. In line with these results, IL-4/GM-CSF-induced fusion was also impaired in DAP12-KI BMM (fig. S2A). Because silencing of DAP12 was induced after macrophage maturation, the data also show that the fusion defect is not mediated by deficient macrophage maturation. To determine if DAP12 is also involved in giant cell formation in the human system, we performed RNA silencing experiments in human monocyte-derived macrophages. With two independent Stealth RNAi constructs, we found that targeted knockdown of DAP12 also reduced IL-4-induced macrophage fusion to levels of the unstimulated control in human macrophages (Fig. 4B). Therefore, DAP12 is required for maximal IL-4-induced macrophage fusion in humans and mice.

Syk deficiency results in impaired macrophage fusion

DAP12 signaling involves recruitment and activation of Syk (19). We therefore asked if Syk is involved in the DAP12-mediated macrophage fusion. Fetal liver-derived macrophages (FLDMs) from Syk-KO embryos (36) were stimulated with IL-4 and GM-CSF to induce macrophage fusion. Whereas WT FLDMs fused efficiently in response to cytokine stimulation, fusion of the Syk-KO FLDMs was barely detectable (Fig. 5). These results are consistent with a requirement for Syk downstream of DAP12 in macrophage fusion.

Targeted knockdown of TREM-2 leads to reduced macrophage fusion

DAP12 is a signaling adaptor protein that pairs with various surface receptors, including TREM-2. Patients with a genetic deficiency in *DAP12* or *TREM-2* present similar symptoms and exhibit similar osteoclast formation defects (15,25). We therefore analyzed the role of TREM-2 in cytokine-induced giant cell formation by monitoring fusion of BMM in which TREM-2 was knocked down with RNAi. Knockdown of TREM-2 led to severely decreased macrophage fusion (Fig. 6). Because the fusion defect was so profound in the TREM-2 knockdown BMM, this receptor appears to play a dominant role during macrophage fusion.

DAP12 overexpression leads to enhanced macrophage fusion

If DAP12 is a key regulator of macrophage fusion, then overexpression of DAP12 should increase giant cell formation. The murine macrophage cell line RAW264.7 did not exhibit sufficient rates of macrophage fusion; therefore, we generated a subclone of this cell line (RAWF) that showed measurable IL-4-induced fusion. The murine DAP12 complementary DNA (cDNA) was cloned into an enhanced green fluorescent protein (EGFP) vector and stable RAWF transfectants were produced expressing either GFP alone (RAWF-EGFP) or the DAP12 GFP fusion protein (RAWF-EGFPDAP12). RAWF cells in which DAP12 was stably overexpressed consistently exhibited higher amounts of spontaneous as well as IL-4-induced macrophage fusion (Fig. 7, A and B).

Deficient DAP12 signaling results in the reduced expression of fusion mediators

Several molecules have been implicated in macrophage fusion. For IL-4-induced giant cell formation, the abundance of the putative seven-transmembrane receptor DC-STAMP and that of the cellular adhesion molecule Cadherin 1 (E-cadherin) are both increased by IL-4 and these proteins participate in macrophage fusion (37,38). To determine if these known fusion molecules are expressed at normal levels in the absence of functional DAP12, we performed semiquantitative real-time reverse transcription polymerase chain reaction (RT-PCR) analysis on ThioMΦ and found that the messenger RNA (mRNA) expression of *DC-STAMP* as well as *Cadherin 1* was severely reduced in IL-4-stimulated and unstimulated DAP12-KI macrophages when compared to the WT control (Fig. 8A). The transcripts for those molecules were also reduced in DAP12-KIBMM (fig. S2B). Although the presence of the DC-STAMP protein was not evaluated because of lack of an appropriate antibody, we did analyze cells for the presence of Cadherin 1 by fluorescence-activated cell sorting (FACS) analysis. In agreement with the reduced mRNA expression in DAP12-KI macrophages, the abundance of Cadherin 1 at the cell surface, both under basal conditions and after exposure to IL-4, was lower in the absence of functional DAP12 (Fig. 8B).

Deficient $\beta 2$ integrin activation in DAP12-deficient macrophages (24) could potentially influence the abundance of fusion mediators. Macrophage adhesion to bacteriologic (untreated polystyrene) plastic is mediated by the $\beta 2$ integrin MAC1 (CD11b/CD18) (39), whereas integrin-independent macrophage adhesion to tissue-culture-treated plastic is mediated by the scavenger receptor SR-A (40). Transcripts for DC-STAMP and Cadherin 1 were reduced in DAP12-KI macrophages plated on either bacteriologic plates or tissue-culture-treated plastic (fig. S3). In addition, the abundance of the transcripts for DC-STAMP and Cadherin 1 was the same as WT for MAC1-KO macrophages plated on bacteriological plastic (Fig. 8C). Thus, the lack of DAP12-mediated signaling appears to alter the gene expression profile of known fusion mediators and this effect is independent of integrin activation or macrophage type.

The fact that the basal and IL-4-induced expression of the genes encoding DC-STAMP and Cadherin 1 was reduced in DAP12-KI macrophages prompted us to analyze the expression of other markers in DAP12 loss-of-function macrophages. Although the abundance of YM1 (also known as chitinase 3-like 3, Chi3l3) and the mannose receptor, which are proteins known to

be induced by IL-4, was the same as that of WT in the DAP12-KI macrophages (Fig. 9A), genome-wide transcriptional analysis revealed that several other IL-4-induced genes were expressed at lower levels in DAP12-KI macrophages (fig. S4). We confirmed by real-time PCR that the abundance of mRNAs for integrin $\beta 3$ (ITGB3), matrix metalloproteinase 13 (MMP13), and heparin-binding epidermal growth factor (EGF)-like growth factor (HBEGF) were reduced in DAP12-deficient macrophages (Fig. 9B). In addition to the reduced transcript levels of these IL-4-regulated genes in DAP12-KI macrophages, we found the expression of other genes to be affected. The mRNA expression and abundance of the innate activation marker MARCO, whose abundance is increased by microbial stimuli in a TLR-dependent manner (41), were higher in the absence of DAP12 signaling (Fig. 9, C and D). The expression of proteins involved in tissue remodeling, such as MMP9 and urokinase plasminogen activator (uPA), were also altered in DAP12-KI macrophages. The mRNA expression of *MMP9* was severely reduced in DAP12-KI macrophages (Fig. 9E), and Western blot analysis and gelatin zymography showed that the reduction in MMP9 was also detectable at the protein level (Fig. 9, F and G). Similar results were found for uPA, mRNA was decreased and casein zymography showed lower uPA activity in cell lysates and supernatants from DAP12-KI macrophages (Fig. 9, H and I). Based on these observations, we conclude that macrophages lacking functional DAP12 display an intrinsically different phenotype from that of WT macrophages. Therefore, we propose that DAP12 is not involved in macrophage maturation but instead influences their programming to produce a fusion-competent phenotype.

DAP12 signaling is required for the formation of foreign body giant cells in vivo

Because macrophage fusion in vitro was severely reduced in the absence of DAP12 signaling, we used a well-established subcutaneous biomaterial implantation model to examine the formation of multinucleated giant cells (42) to ascertain if DAP12 is also required for giant cell formation in vivo. Implantation of biomaterials provokes recruitment of macrophages, which then fuse and form foreign body giant cells on the surface of the implant. We analyzed the foreign body response in DAP12-KI mice at 2 and 4 weeks after implantation. The formation of giant cells was severely compromised in DAP12-KI mice at both time points (Fig. 10, A and B). In addition, the giant cells found around implants of DAP12-KI mice contained fewer nuclei (Fig. 10C). Immunohistochemical detection of macrophages with the MAC3 antibody revealed the presence of numerous macrophages at the implant site, suggesting that macrophage recruitment was not compromised in DAP12-KI mice (Fig. 10D). Thus, a defect in macrophage recruitment cannot account for the reduced number of foreign body giant cells. In fact, enumeration of single macrophages revealed similar abundance between WT and DAP12-KI implants at 4 weeks (38.3 ± 7.1 cells per $300 \mu\text{m}^2$ for WT and 42.1 ± 12.3 cells per $300 \mu\text{m}^2$ for DAP12-KI). These results as well as data from DAP12 gain-of-function transgenic mice expressing multiple copies of DAP12, which exhibit spontaneous formation of multinucleated giant cells in the lung (32), support the conclusion that DAP12 signaling is critical for macrophage fusion in vivo.

DISCUSSION

Multinucleated giant cells are a hallmark of granulomatous inflammation and are formed by fusion of macrophages; however, the detailed mechanism of their formation as well as their function is not known. Here, we show with the use of macrophages from DAP12-KO mice and DAP12-KI (DAP12 with a nonfunctional ITAM motif) loss-of-function mice as well as targeted RNA knockdown in human and mouse macrophages that DAP12 signaling through its ITAM is required for cytokine-induced giant cell formation. Furthermore, we show that the protein tyrosine kinase Syk, which acts downstream of DAP12, and the DAP12-associated receptor TREM-2 are involved in macrophage fusion. Abrogation of DAP12 signaling reduced macrophage fusion, and overexpression of DAP12 enhanced the macrophage fusion. In

agreement with the *in vitro* experiments, DAP12 loss-of-function mice exhibited deficient formation of foreign body giant cells *in vivo*. Because DAP12 gain-of-function transgenic mice expressing multiple copies of DAP12 exhibited spontaneous formation of multinucleated giant cells in the lung (32), we conclude that signaling through DAP12 is not only necessary but also sufficient for giant cell formation *in vitro* and *in vivo*.

The data show that DAP12 signaling plays a decisive role in determining the fusogenic capacity of macrophages. DAP12 is thus not only involved in fusion during osteoclast formation (15, 16,28,29), but is also required for cytokine-induced giant cell formation. Two molecules that have been implicated in macrophage fusion, DC-STAMP and Cadherin 1, were expressed (transcripts and proteins) at lower levels in the absence of DAP12 signaling. Thus, signaling through DAP12 controls the fusogenic capacity of macrophages by regulation of gene transcription. In line with this hypothesis, we found that the expression of a number of genes was affected in DAP12-deficient macrophages. Our pan-genomic transcriptome analysis showed that more than half of the genes up-regulated by IL-4 in WT macrophages were expressed at lower levels in the absence of DAP12 signaling (fig. S4A). In addition, we found that in unstimulated macrophages, more than 700 genes were expressed at lower levels in the absence of DAP12 signaling, whereas more than 500 genes showed a higher expression level when compared to WT macrophages (fig. S4B). These data show that DAP12-deficient macrophages display a phenotype intrinsically different from that of WT macrophages.

Although DC-STAMP and Cadherin 1 have been shown to be involved in macrophage fusion, the decreased abundance of those fusion molecules alone are unlikely to account completely for the striking fusion defect seen in DAP12-KI macrophages. We show here that DAP12 is required on both fusion partners combining to form a giant cell; however, DC-STAMP was found to be required only on one of the fusing macrophages (38). Because the machinery required for macrophage fusion is likely to involve a whole set of known and unknown fusogenic proteins, we hypothesize that DAP12 signaling also controls the expression of unidentified fusion mediators.

Although we used the cytokine IL-4 to induce macrophage fusion *in vitro*, the data show that the role of DAP12 in macrophage fusion appears to be independent of this stimulus. In DAP12-KI and DAP12-KO macrophages, not only was IL-4-induced fusion reduced, but spontaneous macrophage fusion was also reduced. In contrast, DAP12-overexpressing RAW264.7 cells showed higher spontaneous, as well as IL-4-induced, giant cell formation. In agreement with the hypothesis that DAP12's function in programming a fusion-competent state is stimulus independent, we found that most differentially expressed genes were reduced in the presence and in the absence of the IL-4 stimulus. Stimulation by IL-4, therefore, seems to enhance the DAP12-dependent fusion program in macrophages. In addition, we found that DAP12 signaling did not generally influence the IL-4 pathway because IL-4-induced markers, such as YM1 and mannose receptor, were expressed normally in DAP12-KI macrophages. Although IL-4 signal transmission is mainly mediated by Janus kinase (JAK) and signal transducer and activator of transcription 6 (STAT6) signaling, IL-4 can also activate PI3K and stimulate the phosphorylation of Akt (43). Signaling through DAP12 and Syk can also stimulate PI3K activation and Akt phosphorylation and, therefore, may act as a costimulatory signal for regulation of a subset of IL-4-induced genes. It is interesting that DAP12 is required for the IL-4-dependent NK stimulatory capacity of dendritic cells (44). It can be hypothesized that this effect is based on DAP12-mediated regulation of a transcriptional program in dendritic cells.

In addition to the identification of DAP12 as a macrophage fusion regulator, we present evidence that signaling through DAP12 controls gene expression of a range of different molecules. That DAP12-deficient macrophages display global changes in gene expression

suggests that the enhanced TLR responses in the absence of DAP12 demonstrated by others (22) may not be because of a direct effect of DAP12 and TREM-2 on TLR signaling but may be a result of DAP12-dependent macrophage programming. We found several molecules expressed at higher or lower levels in the absence of DAP12 signaling. These include the scavenger receptor MARCO, which was increased in the absence of DAP12 function, and proteins associated with tissue remodeling, such as MMP9 and uPA, which were decreased in the absence of DAP12 function. This further confirms that DAP12 signaling controls macrophage programming, as reflected by expression of factors involved in innate activation, tissue remodeling, and macrophage fusion. Although we show that DAP12 deficiency does not lead to an obvious defect in macrophage numbers or homeostatic functions, this altered macrophage programming may have important implications for infection, wound healing, and antitumor responses.

In humans, mutation of either *DAP12* or *TREM-2* results in PLOSL (also known as Nasu-Hakola syndrome), a rare disease characterized by presenile dementia, bone cysts, and impaired osteoclast differentiation (15,25,45). Our findings suggest that these patients may display additional phenotypes especially when challenged with granulomatous infections.

In macrophages, DAP12 associates with different cell surface receptors. Our results indicate that the DAP12-associated receptor TREM-2 participates in giant cell formation. It has been suggested that TREM-2 can bind to anionic bacterial surface structures (46), but it was shown that macrophages themselves express a TREM-2 ligand (23). The absence of bacteria in our macrophage cultures suggests that during macrophage fusion, signaling through TREM-2 is mediated by the uncharacterized macrophage-associated TREM-2 ligand. In conclusion, signaling through TREM-2, DAP12, and Syk triggers a unique macrophage differentiation pathway, resulting in the programming of macrophages into a fusogenic state through the regulation of gene expression. In line with our findings, DAP12, TREM-2, and Syk have also been associated with the formation of osteoclasts, which are also generated by fusion of macrophages (15,25,28,29,47). Therefore, DAP12 appears to represent a general regulator of macrophage fusion. Our finding that DAP12 mediates macrophage fusion by controlling gene expression is in line with the fact that during osteoclastogenesis, FcR γ and DAP12 are required for the RANKL-mediated induction of NFATc1, which is a transcription factor crucial for RANKL-induced osteoclastogenesis (30). However, the mechanisms by which DAP12 regulates RANKL-induced osteoclast formation and IL-4-induced fusion are likely to be distinct because IL-4 inhibits osteoclast formation and expression of NFATc1 (48).

Overall, the data presented in this study imply a critical role for DAP12 in the formation of multinucleated giant cells and suggest a novel DAP12-dependent pathway of macrophage programming into a fusogenic state. The discovery of DAP12 as a general macrophage fusion regulator represents an important step toward a better understanding of the formation of granuloma-associated multinucleated giant cells. Our work may also pave the way for pharmacological modulation of macrophage fusion through inhibition of protein tyrosine kinases or TREM-2.

MATERIALS AND METHODS

Cytokines and reagents

Recombinant murine GM-CSF and human IL-4 were purchased from Peprotech. Murine IL-4 (mIL-4) was used as a supernatant derived from the mIL-4 cDNA-transfected X63Ag8-653 plasmacytoma transformant cell line (49) cultured in Iscove's modified Dulbecco's medium (IMDM) containing 10% fetal bovine serum (FBS) and penicillin/streptomycin for 4 days. IL-4-containing supernatant was used at a dilution of 1% (v/v) and exhibited only IL-4-specific effects on macrophage fusion (11). We confirmed the specificity of all effects presented in this

paper by using recombinant mIL-4 (R&D Systems) at 20 ng/ml. Antibody against CD18 (GAME-46) was purchased from Santa Cruz and used at a final concentration of 10 µg/ml. Rat antibody against mouse CD11b (5C6) was a gift from P. Taylor (Oxford, UK), rat antibody against mouse F4/80-Alexa647 and isotype control antibodies were purchased from Serotec, rabbit polyclonal antibodies to MMP9 and rat monoclonal antibody to E-cadherin (DECMA-1) from Abcam, and antibody against rat Alexa488 from Invitrogen. Polyclonal rabbit antibodies against mouse YM1 were a gift from G. Krystal, rat antibody against the mannose receptor (5D3) was from L. Martinez-Pomares.

Animals and isolation of murine primary macrophages

All mice used in this study were on a C57BL/6J background, 10 to 30 weeks old, and housed at specific pathogen-free conditions. ThioMΦs and BMMs were isolated as described (11). Fetal liver single-cell suspensions from Syk-KO embryos were a kind gift from E. Schweighoffer and V. Tybulewicz (London, UK). To obtain FLDMs, fetal liver cells were cultured for 6 to 7 days in RPMI 1640 with L-glutamine (Invitrogen) containing 10% heat-inactivated FBS (Biosera, East Sussex, UK), 100 U/ml penicillin and 100 µg/ml streptomycin (P/S, Invitrogen) supplemented with 15% (v/v) L-cell conditioned medium (50) as described for BMM (11).

Fluorescent labeling of primary mouse macrophages

Macrophages were labeled with 5 µM CFSE (Invitrogen) in PBS for 10 min at 37°C. We used the PKH26 Red Fluorescence Cell Linker Kit (Sigma-Aldrich) according to the supplied instructions.

ThioMΦ fusion

ThioMΦ fusion was analyzed as previously described (11). Briefly, labeled ThioMΦs were plated on Permax plastic (eight-well Lab-Tek Chamber Slides, Nunc) in the presence or absence of IL-4 for 24 hours and then fixed with 4% paraformaldehyde (PFA). Imaging analysis was performed with a Zeiss Axioplan upright fluorescence microscope (Plan-Neofluar 10× objective, 0.3 numeric aperture). Three to four independent images were acquired per well, the background was subtracted, and colocalization was measured with MetaMorph software (Molecular Devices).

BMM and FLDM fusion

BMMs or FLDMs were resuspended in OptiMEM containing 10% FBS, P/S and plated on Permax plastic at 1×10^5 macrophages per well. IL-4 and GM-CSF (100 ng/ml) were added and cells were incubated for 2 to 3 days until fusion was maximal. Slides were stained with the Hemacolor staining kit (Merck). Photographs were taken with a Nikon Coolscope slidescanner. Three to four independent images were acquired per well and the number of giant and single-cell nuclei were counted. Percentage fusion was quantified as the number of giant cell nuclei (>2 nuclei) divided by the number of total nuclei.

FACS analysis

Resident peritoneal cell suspensions were collected by peritoneal lavage with PBS. Spleen cell suspensions were prepared by passing spleens through 70-µm cell strainers (BD Biosciences) followed by erythrocyte lysis in 140 mM NH₄Cl/17 mM Tris. For Cadherin 1 FACS, ThioMΦs were plated in the presence or absence of IL-4 on bacteriologic plastic vessels (Greiner) for 24 hours and detached with PBS containing 10 mM EDTA. Cells were blocked (0.5% BSA, 2 mM NaN₃, 5 mM EDTA, 5% goat serum, 5% rabbit serum) and incubated on ice with primary antibodies at 10 µg/ml. Positive staining was detected with antibody against rat Alexa488. Cells were analyzed with a FACSCalibur flow cytometer (BD Biosciences). The

specificity of antibody binding and secondary reagents was monitored through the use of isotype-matched control antibodies (IgG2b for 5C6, IgG1 for DECMA-1).

Immunohistochemistry

Tissue was embedded and frozen in optimal cutting temperature. Frozen tissue sections were thawed at room temperature, fixed in 2% PFA in Hepes-buffered saline, permeabilized in 0.1% Triton X-100 in PBS, quenched with glucose oxidase, blocked in 5% normal goat serum in PBS, and incubated with antibodies against EMR1, CD68, MARCO, and mannose receptor (10 µg/ml). Binding was detected with biotinylated goat antibody against rat immunoglobulin and the horseradish peroxidase (HRP)-avidin and biotinylated enzyme complex (ABC) detection system (Vector Laboratories). The presence of antigen was revealed by incubation with 0.5 mg/ml diaminobenzidine (Polysciences, Inc) and 0.024% H₂O₂ in 10 mmol/l PBS imidazole, pH 7.4. Counterstaining was with methyl green.

Real-time RT-PCR

BMMs or ThioMΦs at 1×10^6 /ml were incubated with or without IL-4 on bacteriologic or tissue-culture-treated six-well vessels for 24 hours. RNA was isolated with the RNeasy Mini Kit (Qiagen), reverse-transcribed with the Quantitect Reverse Transcription Kit (Qiagen). Real-time quantitative PCR was performed on a Rotor-Gene RG3000 (Corbett Research) with the use of the Brilliant SYBR Green QPCR Kit (Stratagene). Expression was normalized to the housekeeping gene *Hprt*. The following primers were used for amplification: *Hprt1*FOR GCTCGAGATGTCATGAAGGAGA, *Hprt1*REV AAAGAACTTATAGCCCCCTTG, *Dcstamp*FOR GTATCGGCTCATCTCCTCCA, *Dcstamp*REV TGCAGCTCGGTTCAAACATA, *Cdh1*FOR CCTGCCAATCCTGATGAAAT, *Cdh1*REV GAACCACTGCCCTCGTAATC, *Hbegf*FOR GACCCATGCCTCAGGAAATA, *Hbegf*REV AGAGTCAGCCCATGACACCT, *Itgb3*FOR GGAACGCTCCATGAAGAAAA, *Itgb3*REV TACAATTCACGGCGTTTTTG, *Mmp13*FOR ACATCCATCCCGTGACCTTA, *Mmp13*REV GCGCTCAGTCTCTTCACCTC, *Mmp9*FOR AGACGACATAGACGGCATCC, *Mmp9*REV GGGACACATAGTGGGAGGTG, *Plau*FOR CAGTGTATGCAGCCCCACTA, *Plau*REV CGGCCTTCGATGTTACAGAT, *Marco*FOR TCGGTTACTCCAGAGGGAGA, *Marco*REV TGCCCCAGGAGTTCTTACTG, *Dap12*FOR: TGCCTTCTGTTCTTCTTCTGT, *Dap12*REV: GGGCATAGAGTGGGCTCAT, *Trem2*FOR: CTGCACTTCAAGGGAAAAGC, *Trem2*REV: CAGTGCTTCAAGGCGTCATA.

Zymography

For analysis of supernatants, ThioMΦs were plated in 24-well tissue culture-treated vessels in serum-free X-Vivo 10 (BioWhittaker) at 2×10^6 cells/ml for 24 hours. Supernatants were concentrated fivefold with YM-10 centrifugal filter devices (Centricon). Cell lysates were prepared in PBS/0.2% Triton X-100. Gelatin zymography was performed as described (51). Briefly, SDS gels contained 1 mg/ml gelatin, type A (Sigma) for gelatin zymography or 2mg/ml casein (Sigma) and 6 µg/ml human plasminogen (Sigma) for casein zymography. Gels were renatured in 2.5% Triton X-100 and incubated in 200 mM NaCl, 40 mM Tris-HCl, pH 7.5, 10 mM CaCl₂, 1 µM ZnCl₂ for gelatin zymography or in 0.1 M Tris, pH 8.0 for casein zymography at 37°C and stained with Coomassie blue.

Western blot analysis

Cells were lysed in protein lysis buffer [20 mM Tris-HCl, pH 7.5, 140 mM NaCl, 1 mM EDTA, 1% NP40, 1 mM Na₃VO₄, and proteinase inhibitor cocktail (Complete Mini, Roche)] and lysates were loaded onto 10% SDS gels. Gels were blotted onto polyvinylidene difluoride membranes (GE Healthcare), membranes were blocked in Tris-buffered saline, 0.1%

Tween-20, and 5% milk powder and incubated with antibody against MMP9 overnight. Peroxidase-conjugated antibody against rat IgG (Jackson Immunoresearch Laboratories) was used as secondary antibody and signals were detected with the ECL kit (GE Healthcare).

Isolation of the fusogenic RAW267.4 clone RAWF

RAW264.7 (ATCC) cells were plated at limiting dilution in 96-well plates, grown, and tested for fusogenicity by addition of IL-4. One fusogenic clone was selected and recloned.

Cloning and transfection

Murine *DAP12* cDNA was amplified with the following primers: Forward primer AAGCTAGCCCCGCCATGGGGGCTCTGGAGCCCTCC, reverse primer AACACACAGAGGCAATATTACCAGTCGACAA and cloned into pEYFP-N1 (BD Biosciences, Franklin Lakes, US) via the *NheI* and *SalI* site. Transfections were performed with FuGene6 (Roche). Stable transfectants were selected by prolonged culture in medium containing G418 at 600 to 1000 $\mu\text{g/ml}$.

Preparation of human macrophages

Human monocytes were isolated from buffy coats from healthy donors (Bristol Blood Donor Services). Peripheral blood mononuclear cells were isolated by centrifugation over a Ficoll gradient and monocytes were isolated by selective adherence to gelatin-coated plates. After 18 hours adherence, monocytes were detached and cultured in X-Vivo 10 supplemented with 10% autologous serum for 4 days to obtain human macrophages.

Targeted knockdown with Stealth RNAi

Human or murine macrophages were plated on Permax eight-well chamber slides and allowed to adhere. RNA silencing was performed with the INTERFERin small interfering RNA transfection reagent (Polyplus-transfection, Inc.) according to the supplied instructions. Stealth RNAi for mDAP12, mTREM-2, and hDAP12 and Stealth universal control were from Invitrogen and used at a final concentration of 10 nM. After 24 hours, IL-4 or IL-4/GM-CSF cells were added and the cells were stained with Hemacolor 24 to 36 hours later when fusion in the control was maximal. Percentage fusion was quantified as the number of giant cell nuclei (>2 nuclei) divided by the total number of nuclei. The following RNAi sequences were used: mDAP12, UGCUGAGACUGAGUCGCCUUAUCAG; mTREM-2, UGUGCUCUCCAUUCCGCUUCUUCAGG; hDAP12 RNAi 1, GCCCAGAGCGAUUGCAGUUGCUCUA; hDAP12 RNAi 2, CCGAGUCGCCUUAUCAGGAGCUCCA

Implantation of biomaterials

All procedures were performed in accordance with the regulations adopted by the National Institutes of Health and approved by the Animal Care and Use Committee of Yale University. Subcutaneous implantations of Millipore filters composed of mixed cellulose esters was performed essentially as described previously (42). Twelve DAP12-KI and 12 control mice (C57BL/6), age 3 to 4 months, were used for implantations. Each mouse received two implants that were placed at least 2 cm apart. Implants were excised en bloc at 2 and 4 weeks after implantation and processed for histological and immunohistochemical analysis according to standard protocols. Macrophage recruitment and foreign body giant cell formation were evaluated in sections stained with the Mac-3 antibody as described previously (42).

Supplementary Material

Refer to Web version on PubMed Central for supplementary material.

REFERENCES AND NOTES

1. Langhans T. Ueber Riesenzellen mit wandständigen Kernen in Tuberkeln und die fibröse Form des Tuberkels. *Virchows Arch. Pathol. Anat* 1868;42:382–404.
2. Anderson JM. Multinucleated giant cells. *Curr. Opin. Hematol* 2000;7:40–47. [PubMed: 10608503]
3. Helming L, Gordon S. The molecular basis of macrophage fusion. *Immunobiology* 2008;212:785–793. [PubMed: 18086379]
4. Chambers TJ, Spector WG. Inflammatory giant cells. *Immunobiology* 1982;161:283–289. [PubMed: 7047375]
5. Chen EH, Grote E, Mohler W, Vignery A. Cell—cell fusion. *FEBS Lett* 2007;581:2181–2193. [PubMed: 17395182]
6. Huppertz B, Bartz C, Kokozidou M. Trophoblast fusion: Fusogenic proteins, syncytins and ADAMS, and other prerequisites for syncytial fusion. *Micron* 2006;37:509–517. [PubMed: 16497505]
7. Zhao Q, Topham N, Anderson JM, Hiltner A, Lodoen G, Payet CR. Foreign-body giant cells and polyurethane biostability: In vivo correlation of cell adhesion and surface cracking. *J. Biomed. Mater. Res* 1991;25:177–183. [PubMed: 2055915]
8. Byrd TF. Multinucleated giant cell formation induced by IFN-gamma/IL-3 is associated with restriction of virulent *Mycobacterium tuberculosis* cell to cell invasion in human monocyte monolayers. *Cell Immunol* 1998;188:89–96. [PubMed: 9756638]
9. Zhu XW, Price NM, Gilman RH, Recarvarren S, Friedland JS. Multinucleate giant cells release functionally unopposed matrix metalloproteinase-9 in vitro and in vivo. *J. Infect. Dis* 2007;196:1076–1079. [PubMed: 17763331]
10. Vignery A. Macrophage fusion: The making of osteoclasts and giant cells. *J. Exp. Med* 2005;202:337–340. [PubMed: 16061722]
11. Helming L, Gordon S. Macrophage fusion induced by IL-4 alternative activation is a multistage process involving multiple target molecules. *Eur. J. Immunol* 2007;37:33–42. [PubMed: 17154265]
12. Olcese L, Cambiaggi A, Semenzato G, Bottino C, Moretta A, Vivier E. Human killer cell activatory receptors for MHC class I molecules are included in a multimeric complex expressed by natural killer cells. *J. Immunol* 1997;158:5083–5086. [PubMed: 9164921]
13. Tomasello E, Olcese L, Vely F, Geourgeon C, Blery M, Moqrich A, Gautheret D, Djabali M, Mattei MG, Vivier E. Gene structure, expression pattern, and biological activity of mouse killer cell activating receptor-associated protein (KARAP)/DAP-12. *J. Biol. Chem* 1998;273:34115–34119. [PubMed: 9852069]
14. Lanier LL, Corliss BC, Wu J, Leong C, Phillips JH. Immunoreceptor DAP12 bearing a tyrosine-based activation motif is involved in activating NK cells. *Nature* 1998;391:703–707. [PubMed: 9490415]
15. Paloneva J, Mandelin J, Kiialainen A, Bohling T, Prudlo J, Hakola P, Haltia M, Kontinen YT, Peltonen L. DAP12/TREM2 deficiency results in impaired osteoclast differentiation and osteoporotic features. *J. Exp. Med* 2003;198:669–675. [PubMed: 12925681]
16. Kaifu T, Nakahara J, Inui M, Mishima K, Momiyama T, Kaji M, Sugahara A, Koito H, Ujike-Asai A, Nakamura A, Kanazawa K, Tan-Takeuchi K, Iwasaki K, Yokoyama WM, Kudo A, Fujiwara M, Asou H, Takai T. Osteopetrosis and thalamic hypomyelinoses with synaptic degeneration in DAP12-deficient mice. *J. Clin. Invest* 2003;111:323–332. [PubMed: 12569157]
17. Lanier LL, Bakker AB. The ITAM-bearing transmembrane adaptor DAP12 in lymphoid and myeloid cell function. *Immunol. Today* 2000;21:611–614. [PubMed: 11114420]
18. Tomasello E, Vivier E. KARAP/DAP12/TYROBP: Three names and a multiplicity of biological functions. *Eur. J. Immunol* 2005;35:1670–1677. [PubMed: 15884055]
19. Turnbull IR, Colonna M. Activating and inhibitory functions of DAP12. *Nat. Rev. Immunol* 2007;7:155–161. [PubMed: 17220916]
20. Vivier E, Nunes JA, Vely F. Natural killer cell signaling pathways. *Science* 2004;306:1517–1519. [PubMed: 15567854]
21. Tessarz AS, Cerwenka A. The TREM-1/DAP12 pathway. *Immunol. Lett* 2008;116:111–116. [PubMed: 18192027]
22. Hamerman JA, Tchao NK, Lowell CA, Lanier LL. Enhanced Toll-like receptor responses in the absence of signaling adaptor DAP12. *Nat. Immunol* 2005;6:579–586. [PubMed: 15895090]

23. Hamerman JA, Jarjoura JR, Humphrey MB, Nakamura MC, Seaman WE, Lanier LL. Cutting edge: Inhibition of TLR and FcR responses in macrophages by triggering receptor expressed on myeloid cells (TREM)-2 and DAP12. *J. Immunol* 2006;177:2051–2055. [PubMed: 16887962]
24. Mocsai A, Abram CL, Jakus Z, Hu Y, Lanier LL, Lowell CA. Integrin signaling in neutrophils and macrophages uses adaptors containing immunoreceptor tyrosine-based activation motifs. *Nat. Immunol* 2006;7:1326–1333. [PubMed: 17086186]
25. Paloneva J, Kestila M, Wu J, Salminen A, Bohling T, Ruotsalainen V, Hakola P, Bakker AB, Phillips JH, Pekkarinen P, Lanier LL, Timonen T, Peltonen L. Loss-of-function mutations in TYROBP (DAP12) result in a presenile dementia with bone cysts. *Nat. Genet* 2000;25:357–361. [PubMed: 10888890]
26. Bakker AB, Hoek RM, Cerwenka A, Blom B, Lucian L, McNeil T, Murray R, Phillips LH, Sedgwick JD, Lanier LL. DAP12-deficient mice fail to develop autoimmunity due to impaired antigen priming. *Immunity* 2000;13:345–353. [PubMed: 11021532]
27. Tomasello E, Desmoulins PO, Chemin K, Guia S, Cremer H, Ortaldo J, Love P, Kaiserlian D, Vivier E. Combined natural killer cell and dendritic cell functional deficiency in KARAP/DAP12 loss-of-function mutant mice. *Immunity* 2000;13:355–364. [PubMed: 11021533]
28. Nataf S, Anginot A, Vuaillet C, Malaval L, Fodil N, Chereul E, Langlois JB, Dumontel C, Cavillon G, Confavreux C, Mazzorana M, Vico L, Belin MF, Vivier E, Tomasello E, Jurdic P. Brain and bone damage in KARAP/DAP12 loss-of-function mice correlate with alterations in microglia and osteoclast lineages. *Am. J. Pathol* 2005;166:275–286. [PubMed: 15632019]
29. Humphrey MB, Ogasawara K, Yao W, Spusta SC, Daws MR, Lane NE, Lanier LL, Nakamura MC. The signaling adapter protein DAP12 regulates multinucleation during osteoclast development. *J. Bone Miner. Res* 2004;19:224–234. [PubMed: 14969392]
30. Koga T, Inui M, Inoue K, Kim S, Suematsu A, Kobayashi E, Iwata T, Ohnishi H, Matozaki T, Kodama T, Taniguchi T, Takayanagi H, Takai T. Costimulatory signals mediated by the ITAM motif cooperate with RANKL for bone homeostasis. *Nature* 2004;428:758–763. [PubMed: 15085135]
31. Zou W, Kitaura H, Reeve J, Long F, Tybulewicz VL, Shattil SJ, Ginsberg MH, Ross FP, Teitelbaum SL. Syk, c-Src, the alphavbeta3 integrin, and ITAM immunoreceptors, in concert, regulate osteoclastic bone resorption. *J. Cell Biol* 2007;176:877–888. [PubMed: 17353363]
32. Lucas M, Daniel L, Tomasello E, Guia S, Horschowski N, Aoki N, Figarella-Branger D, Gomez S, Vivier E. Massive inflammatory syndrome and lymphocytic immunodeficiency in KARAP/DAP12-transgenic mice. *Eur. J. Immunol* 2002;32:2653–2663. [PubMed: 12207350]
33. Aoki N, Kimura S, Takiyama Y, Atsuta Y, Abe A, Sato K, Katagiri M. The role of the DAP12 signal in mouse myeloid differentiation. *J Immunol* 2000;165:3790–3796. [PubMed: 11034384]
34. McNally AK, Anderson JM. Beta1 and beta2 integrins mediate adhesion during macrophage fusion and multinucleated foreign body giant cell formation. *Am. J. Pathol* 2002;160:621–630. [PubMed: 11839583]
35. Jay SM, Skokos E, Laiwalla F, Krady MM, Kyriakides TR. Foreign body giant cell formation is preceded by lamellipodia formation and can be attenuated by inhibition of Rac1 activation. *Am. J. Pathol* 2007;171:632–640. [PubMed: 17556592]
36. Turner M, Mee PJ, Costello PS, Williams O, Price AA, Duddy LP, Furlong MT, Geahlen RL, Tybulewicz VL. Perinatal lethality and blocked B-cell development in mice lacking the tyrosine kinase Syk. *Nature* 1995;378:298–302. [PubMed: 7477352]
37. Moreno JL, Mikhaïlenko I, Tondravi MM, Keegan AD. IL-4 promotes the formation of multinucleated giant cells from macrophage precursors by a STAT6-dependent, homotypic mechanism: Contribution of E-cadherin. *J. Leukoc. Biol* 2007;82:1542–1553. [PubMed: 17855502]
38. Yagi M, Miyamoto T, Sawatani Y, Iwamoto K, Hosogane N, Fujita N, Morita K, Ninomiya K, Suzuki T, Miyamoto K, Oike Y, Takeya M, Toyama Y, Suda T. DC-STAMP is essential for cell—cell fusion in osteoclasts and foreign body giant cells. *J. Exp. Med* 2005;202:345–351. [PubMed: 16061724]
39. Rosen H, Gordon S. Monoclonal antibody to the murine type 3 complement receptor inhibits adhesion of myelomonocytic cells in vitro and inflammatory cell recruitment in vivo. *J. Exp. Med* 1987;166:1685–1701. [PubMed: 2445894]
40. Fraser I, Hughes D, Gordon S. Divalent cation-independent macrophage adhesion inhibited by monoclonal antibody to murine scavenger receptor. *Nature* 1993;364:343–346. [PubMed: 8332192]

41. Mukhopadhyay S, Chen Y, Sankala M, Peiser L, Pikkarainen T, Kraal G, Tryggvason K, Gordon S. MARCO, an innate activation marker of macrophages, is a class A scavenger receptor for *Neisseria meningitidis*. *Eur. J. Immunol* 2006;36:940–949. [PubMed: 16525990]
42. Kyriakides TR, Foster MJ, Keeney GE, Tsai A, Giachelli CM, Clark-Lewis I, Rollins BJ, Bornstein P. The CC chemokine ligand, CCL2/MCP1, participates in macrophage fusion and foreign body giant cell formation. *Am. J. Pathol* 2004;165:2157–2166. [PubMed: 15579457]
43. Jiang H, Harris MB, Rothman P. IL-4/IL-13 signaling beyond JAK/STAT. *J. Allergy Clin. Immunol* 2000;105:1063–1070. [PubMed: 10856136]
44. Terme M, Tomasello E, Maruyama K, Crepineau F, Chaput N, Flament C, Marolleau JP, Angevin E, Wagner EF, Salomon B, Lemonnier FA, Wakasugi H, Colonna M, Vivier E, Zitvogel L. IL-4 confers NK stimulatory capacity to murine dendritic cells: A signaling pathway involving KARAP/DAP12-triggering receptor expressed on myeloid cell 2 molecules. *J. Immunol* 2004;172:5957–5966. [PubMed: 15128777]
45. Paloneva J, Manninen T, Christman G, Hovanes K, Mandelin J, Adolfsson R, Bianchin M, Bird T, Miranda R, Salmaggi A, Tranebjaerg L, Kontinen Y, Peltonen L. Mutations in two genes encoding different subunits of a receptor signaling complex result in an identical disease phenotype. *Am. J. Hum. Genet* 2002;71:656–662. [PubMed: 12080485]
46. Daws MR, Sullam PM, Niemi EC, Chen TT, Tchao NK, Seaman WE. Pattern recognition by TREM-2: Binding of anionic ligands. *J. Immunol* 2003;171:594–599. [PubMed: 12847223]
47. Humphrey MB, Daws MR, Spusta SC, Niemi EC, Torchia JA, Lanier LL, Seaman WE, Nakamura MC. TREM2, a DAP12-associated receptor, regulates osteoclast differentiation and function. *J. Bone Miner. Res* 2006;21:237–245. [PubMed: 16418779]
48. Kamel Mohamed SG, Sugiyama E, Shinoda K, Hounoki H, Taki H, Maruyama M, Miyahara T, Kobayashi M. Interleukin-4 inhibits RANKL-induced expression of NFATc1 and c-Fos: A possible mechanism for downregulation of osteoclastogenesis. *Biochem. Biophys. Res. Commun* 2005;329:839–845. [PubMed: 15752732]
49. Karasuyama H, Melchers F. Establishment of mouse cell lines which constitutively secrete large quantities of interleukin 2, 3, 4 or 5, using modified cDNA expression vectors. *Eur. J. Immunol* 1988;18:97–104. [PubMed: 2831066]
50. Hume DA, Gordon S. Optimal conditions for proliferation of bone marrow-derived mouse macrophages in culture: The roles of CSF-1, serum, Ca²⁺, and adherence. *J. Cell Physiol* 1983;117:189–194. [PubMed: 6605349]
51. Herron GS, Banda MJ, Clark EJ, Gavrilovic J, Werb Z. Secretion of metalloproteinases by stimulated capillary endothelial cells. II. Expression of collagenase and stromelysin activities is regulated by endogenous inhibitors. *J. Biol. Chem* 1986;261:2814–2818. [PubMed: 3005266]
52. We thank E. Schweighoffer and V. Tybulewicz for providing *syk*-KO fetal livers, R. Stillion for performing immunohistochemistry, and E. A. Skokos and W. Tian for assistance with the implantation studies. This work was supported by the German Research Foundation (DFG), the Medical Research Council, and the NIH Grant GM 072194-01 (to T.R.K.). E.V. laboratory is supported by INSERM, CNRS, the European Community (ALLOSTEM), Ligue Nationale contre le Cancer (“Equipe labellisée La Ligue”), the Agence Nationale de la Recherche (“Réseau Innovation Biotechnologies”; “Microbiologie Immunologie—Maladies Emergentes”; “Maladies Rares”; “Plates-Formes Technologiques du Vivant”), Institut National du Cancer, Ministère de l’Enseignement Supérieur et de la Recherche. E.V. is a scholar of the Institut Universitaire de France. E.V. is a founder, consultant, and shareholder of Innate-Pharma.

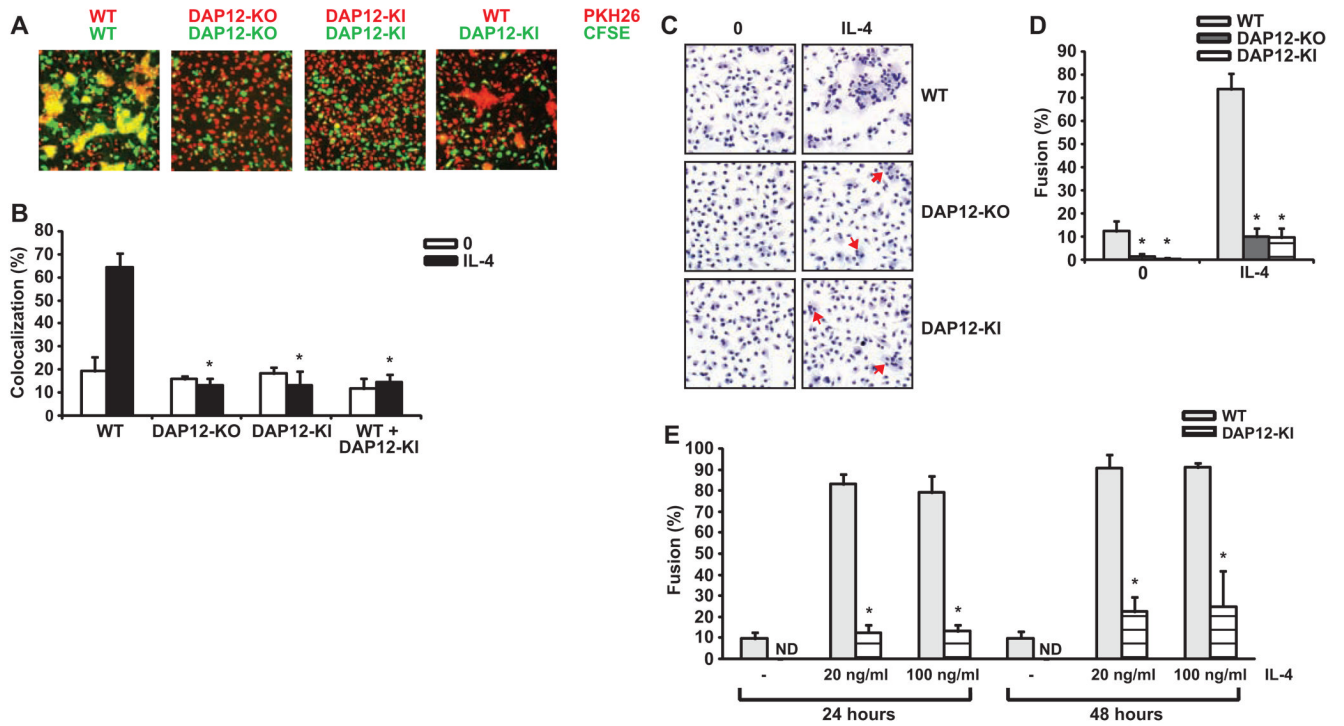


Fig. 1. DAP12 deficiency results in impaired macrophage fusion. (A) ThioMΦ from wild-type (WT), DAP12-deficient (DAP12-KO), and DAP12 loss-of-function (DAP12-KI) mice were labeled with CFSE and PKH26 and fusion was induced by exposure to IL-4 for 24 hours. Macrophage fusion is represented by colocalization of the red and green fluorescent labels (yellow). (B) Quantitation of colocalization. Shown are means \pm SD of five measurements; * $P = 0.0121$, Mann-Whitney test, two-tailed (compared to WT in the presence of IL-4). Shown is a representative of three independent experiments. (C) Hemacolor staining of unstimulated or ThioMΦ stimulated with IL-4. Some small multinucleated giant cells are visible in IL-4-treated DAP12-KO and DAP12-KI macrophages (red arrows). (D) Macrophage fusion was quantified as the percentage of giant cell nuclei relative to the total number of nuclei. Shown are means \pm SD of nine measurements combined from three independent experiments, * $P = 0.0004$ (Mann-Whitney test, two-tailed). (E) Macrophage fusion, quantified as in (D) after stimulation with 20 or 100 ng/ml IL-4 and incubation for 24 or 48 hours. Shown are means \pm SD of six measurements combined from two independent experiments, * $P = 0.0051$ (Mann-Whitney test, two-tailed).

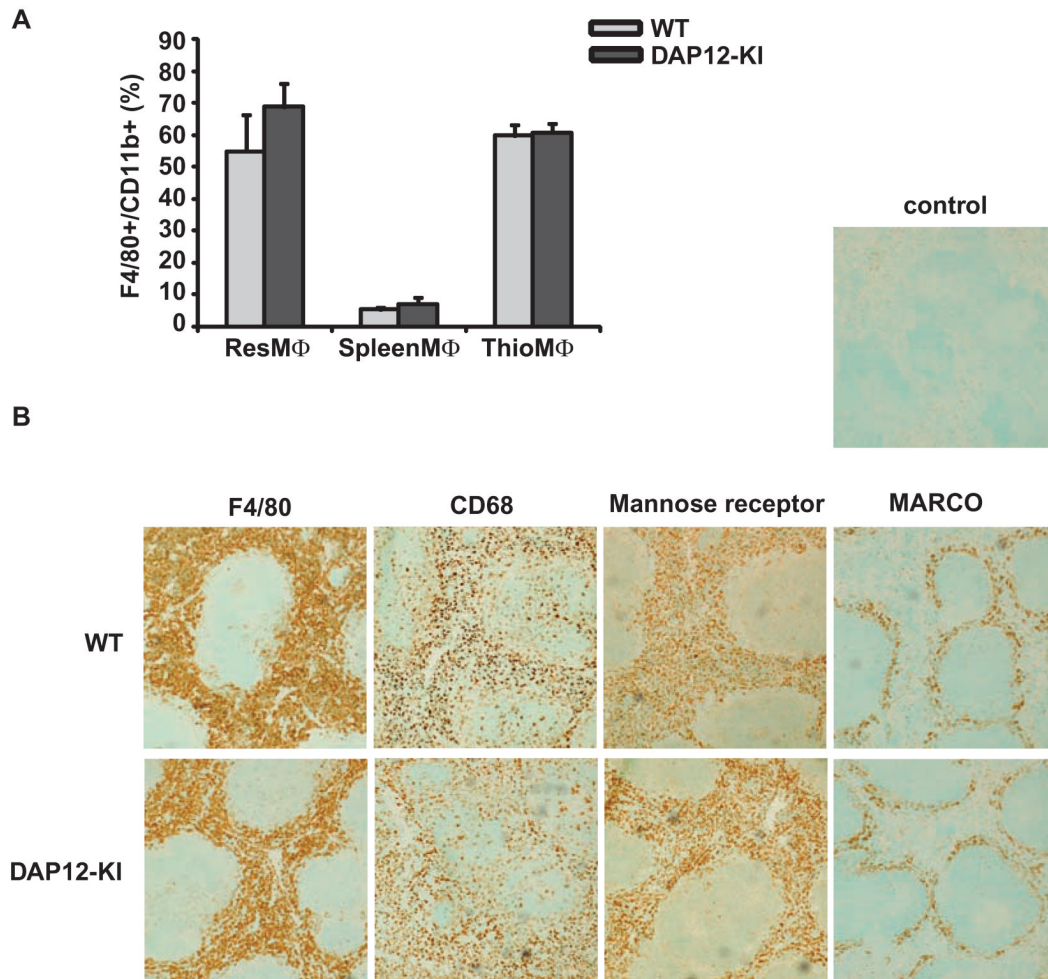
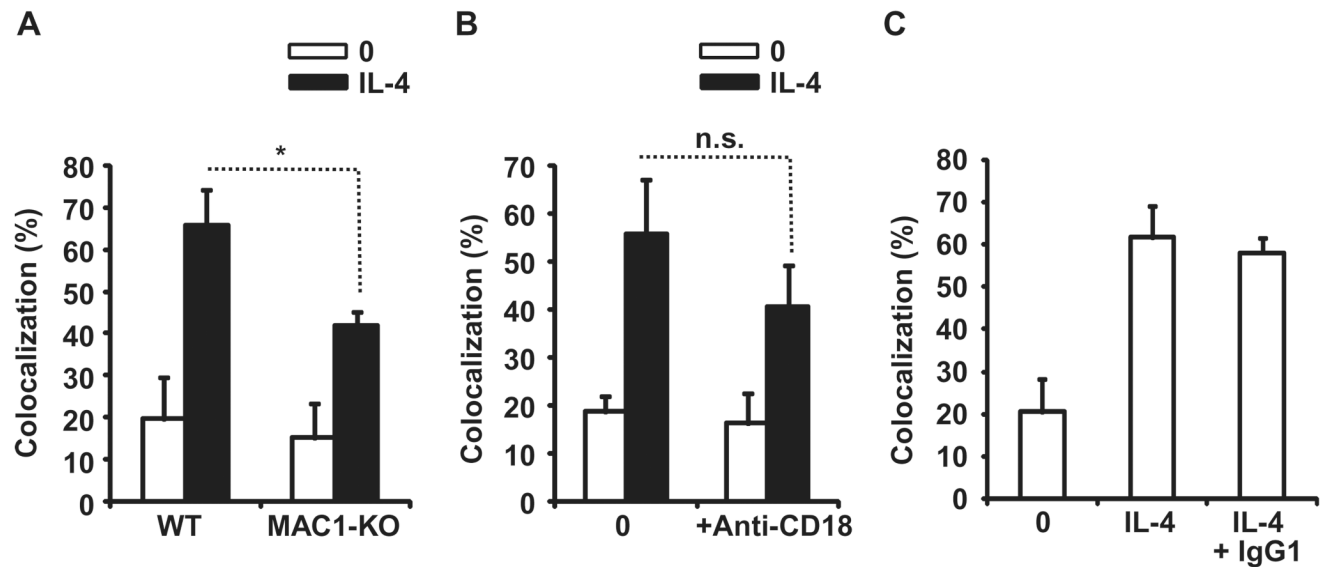


Fig. 2. Macrophage differentiation is normal in DAP12-KI mice. **(A)** Percentages of F4/80 and CD11b double-positive cells (F4/80+/CD11b+) were determined by FACS analysis of cells from the peritoneal cavity (resident peritoneal macrophage, resMΦ), the spleen (SpleenMΦ), and the peritoneal cavity 4 days after thioglycollate injection (ThioMΦ). Shown are means \pm SD from three animals. **(B)** Frozen sections of spleens from WT and DAP12-KI mice were stained with F4/80, FA11 (CD68), 5D3 (mannose receptor), and ED31 (MARCO); staining was detected with HRP-conjugated secondary antibodies and nuclei were counterstained with methyl green. Control, secondary antibody.

**Fig. 3.**

Macrophage fusion is only partially dependent on $\beta 2$ integrin activation. (A) ThioM Φ from WT and MAC1-KO mice were labeled with CFSE and PKH26 and fusion was induced by exposure to IL-4. Macrophage fusion is represented by the percentage of colocalization of the red and green fluorescent labels. Shown are means \pm SD of six measurements combined from two independent experiments. * $P = 0.0051$ (Mann-Whitney test, two-tailed). (B) ThioM Φ fusion in the presence of antibodies against CD18. Shown are means \pm SD of four measurements, n.s., not significant. Similar results were obtained in two independent experiments. (C) ThioM Φ fusion in the presence of IgG1 isotype control antibodies. Shown are means \pm SD of three measurements. Similar results were obtained in two independent experiments.

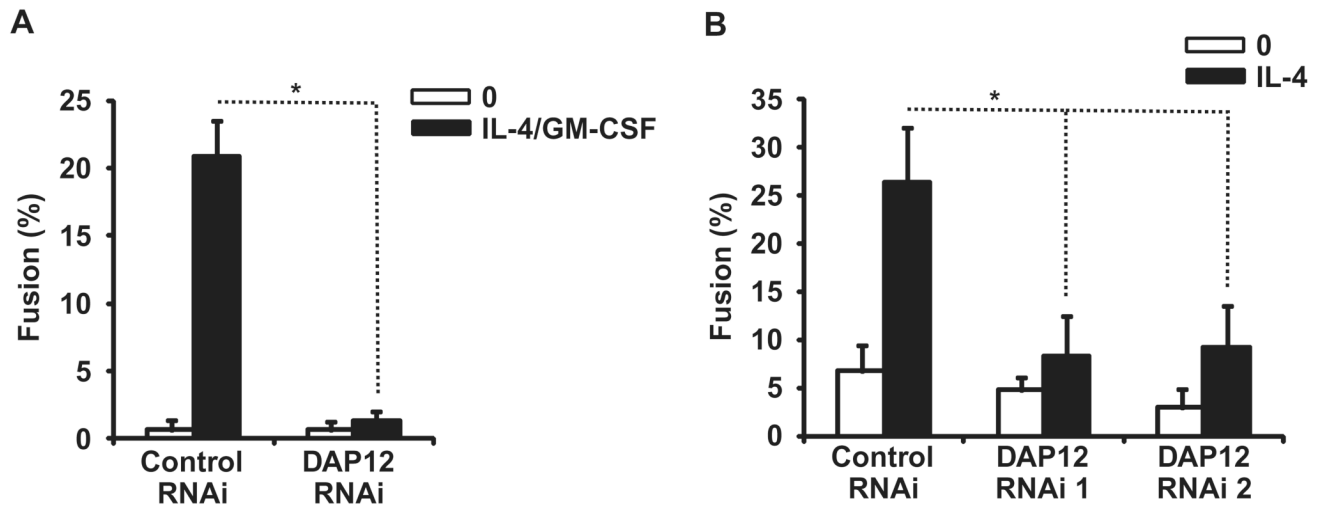


Fig. 4. Targeted DAP12 knockdown leads to reduced IL-4-induced macrophage fusion. **(A)** Adherent BMMs were transfected with Stealth mDAP12 RNAi and fusion was induced by addition of IL-4 and GM-CSF 24 hours later. Macrophage fusion was quantified as the percentage of giant cell nuclei relative to the total number of nuclei. Shown are means \pm SD of eight measurements. DAP12 knockdown led to a significant reduction in DAP12 mRNA levels after 24 hours (2.4-fold, $P \leq 0.05$, determined by real-time PCR from three independent experiments). **(B)** Adherent human monocyte-derived macrophages were transfected with two different Stealth hDAP12 RNAi duplexes (RNAi 1, RNAi 2) and fusion was induced by addition of IL-4 24 hours later. Macrophage fusion was quantified as in (A). Shown are means \pm SD of eight measurements combined from two donors. (A and B) $*P = 0.0009$ (Mann-Whitney test, two-tailed); results were confirmed in three independent experiments.

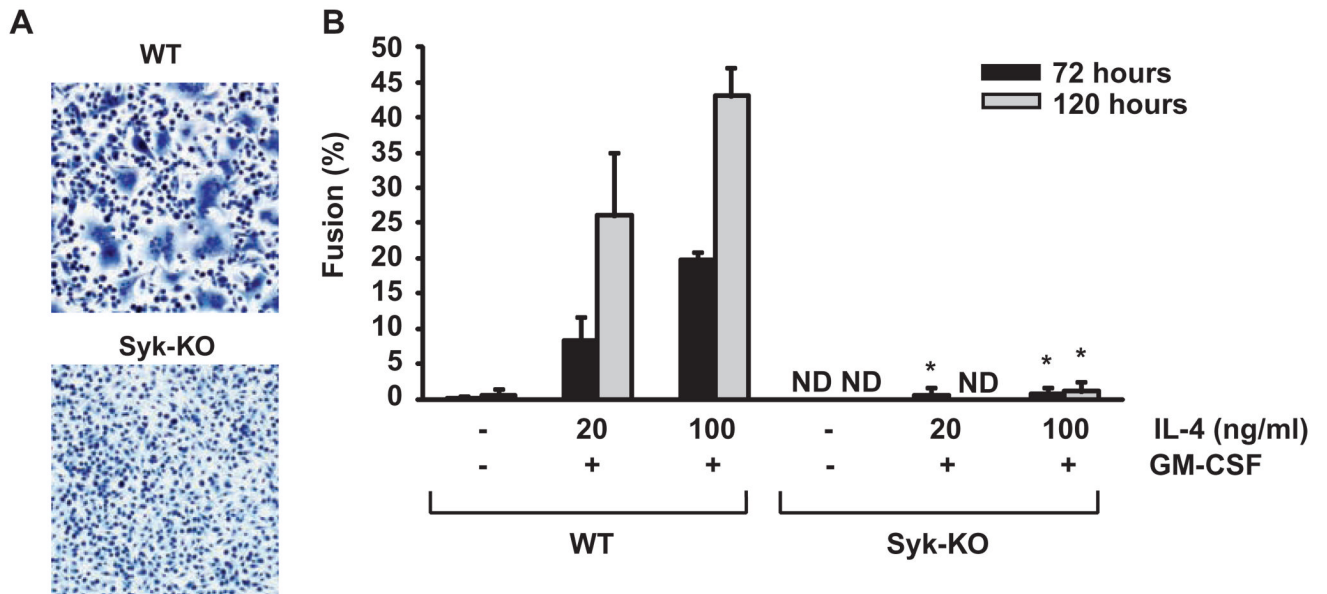


Fig. 5. Syk deficiency results in reduced IL-4- and GM-CSF-induced macrophage fusion. FLDM from WT and Syk-KO embryonic livers were stimulated with IL-4 and GM-CSF to induce macrophage fusion. **(A)** Hemacolor staining. **(B)** Macrophage fusion quantified after stimulation with 20 or 100 ng/ml IL-4 and incubation for 72 or 120 hours. Fusion was measured as the percentage of giant cell nuclei relative to the total number of nuclei [= Fusion (%)]; ND, not detectable. Shown are means \pm SD of six measurements combined from two independent experiments; * $P = 0.0051$ (compared to WT, Mann-Whitney test, two-tailed).

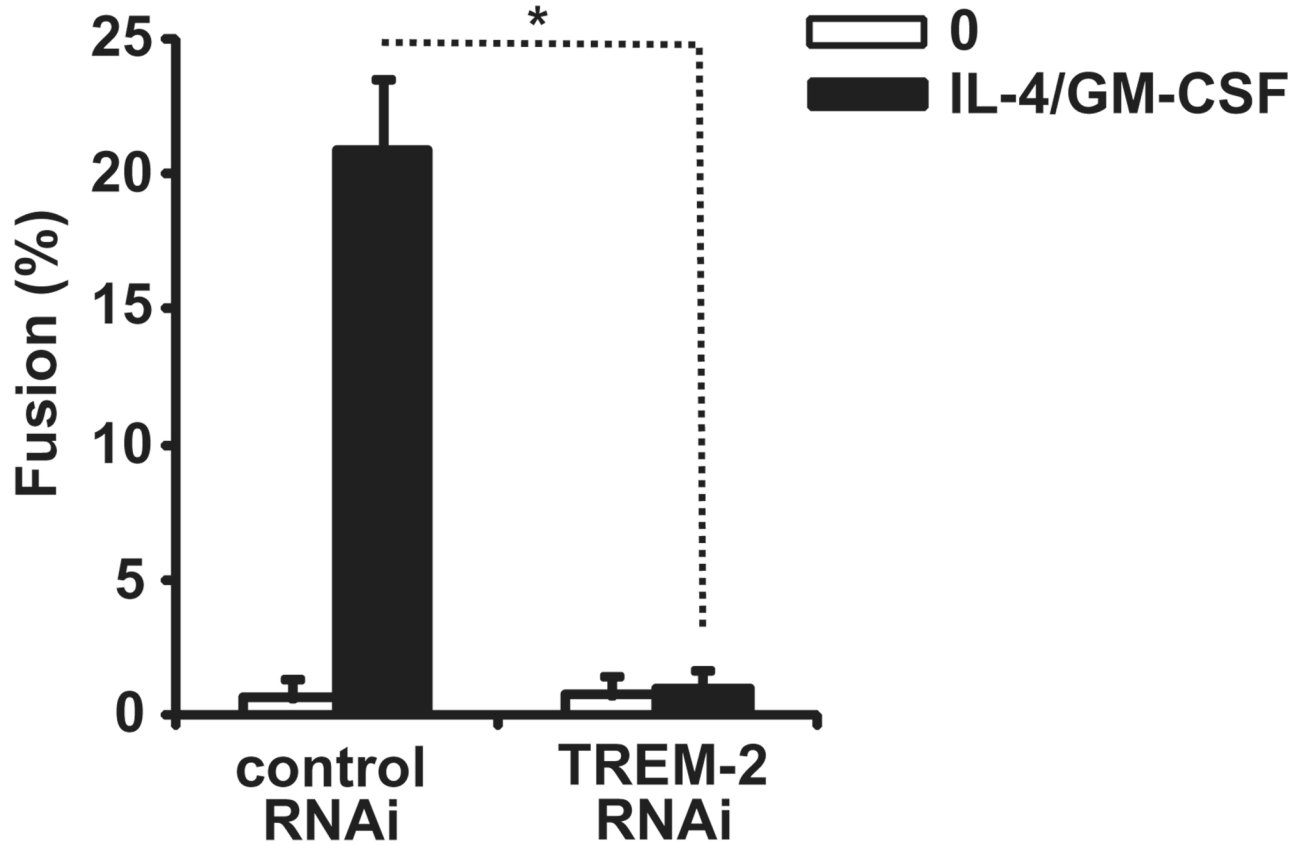


Fig. 6.

Targeted TREM-2 knockdown leads to reduced IL-4 induced macrophage fusion. Adherent BMMs were transfected with Stealth TREM-2 RNAi and fusion was induced by addition of IL-4 and GM-CSF 24 hours later. Fusion was quantified as the percentage of giant cell nuclei relative to the total number of nuclei. Shown are means \pm SD of eight measurements; $*P = 0.0009$ (Mann-Whitney test, two-tailed). Results were confirmed in three independent experiments. TREM-2 knockdown led to a significant reduction in TREM-2 mRNA concentrations after 24 hours (2.2-fold, $P \leq 0.05$, determined by real-time PCR from three independent experiments).

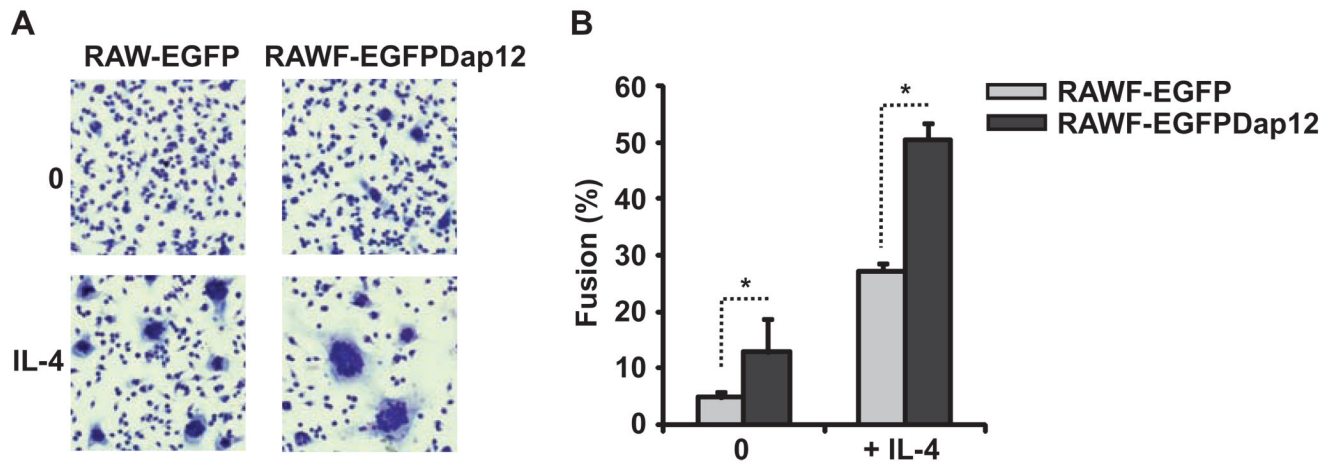
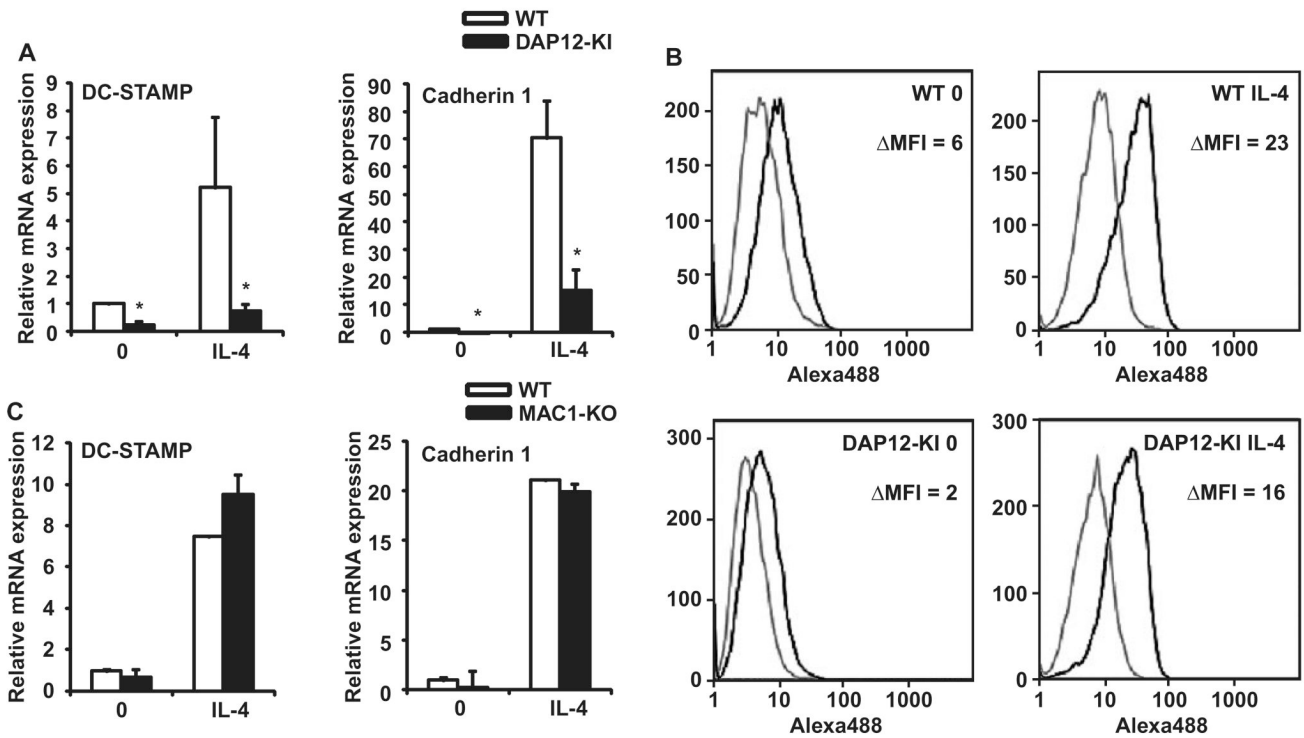


Fig. 7. DAP12 overexpression in fusogenic RAW264.7 macrophages leads to enhanced fusion. A fusogenic subclone of the cell line RAW264.7 (RAWF) was stably transfected with an empty EGFP vector (RAWF-EGFP) or with an EGFP vector containing DAP12 cDNA (RAWF-EGFPDAP12). Stable transfectants were cultured in the presence or absence of IL-4 for 24 hours. **(A)** Hemacytometer staining. **(B)** Quantitation of macrophage fusion. Fusion was quantified as the percentage of giant cell nuclei relative to the total number of nuclei. Shown are means \pm SD of four measurements; * $P \leq 0.05$ (Mann-Whitney test, two-tailed). Similar results were obtained in three independent experiments. Real-time PCR analysis of DAP12 expression in RAWF-EGFP and RAWF-EGFP-DAP12 cells showed that DAP12 mRNA was significantly increased (2.2-fold, $P \leq 0.05$, measurements combined from three independent experiments).

**Fig. 8.**

Reduced expression of fusion mediators in DAP12-KI macrophages. (A) WT and DAP12-KI ThioM Φ s were cultured in the presence or absence of IL-4 for 24 hours. RNA was isolated and analyzed by real-time PCR for DC-STAMP and Cadherin 1 expression. Expression was normalized to a housekeeping gene (*Hprt*) as well as the unstimulated WT control. Shown are means \pm SD of measurements from four (DC-STAMP) or three (Cadherin 1) independent experiments. * $P \leq 0.05$ (compared to WT, Student's *t* test, two-tailed). (B) ThioM Φ s were stimulated with or without IL-4 for 24 hours on bacteriologic plastic, fixed, stained with antibodies against E-cadherin and secondary Alexa488-labeled antibodies, and analyzed by FACS. MFI, mean fluorescence intensity. Abundance was quantified as Δ MFI = $MFI_{E-cadherin} - MFI_{IgG1}$. Experiments were performed three times with similar results. (C) Real-time PCR analysis of DC-STAMP and Cadherin 1 expression in WT and MAC1-KO ThioM Φ . Shown are means \pm SD of measurements. Results were confirmed in two independent experiments.

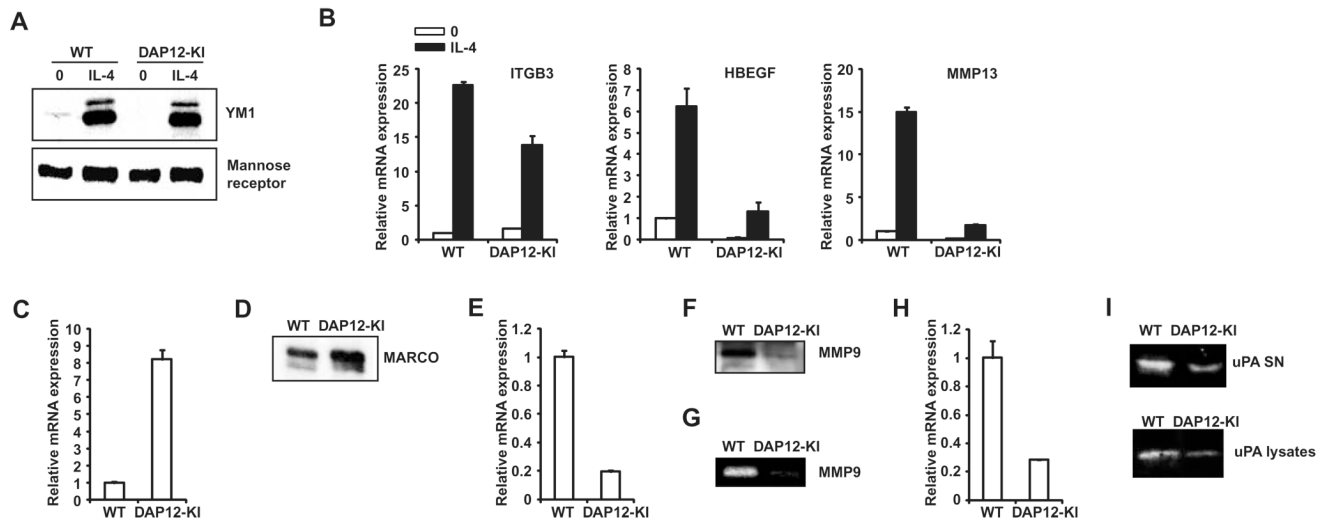


Fig. 9. Macrophage programming is affected in the absence of DAP12 signaling. **(A)** Lysates from WT and DAP12-KI ThioM Φ incubated with or without IL-4 for 24 hours were subjected to Western blot analysis. Results were confirmed twice. **(B)** Real-time PCR analysis of the expression of β 3 integrin (ITGB3), heparin-binding EGF-like growth factor (HBEGF), and matrix metalloproteinase 13 (MMP13) in ThioM Φ as described in Fig. 8A. **(C)** Real-time PCR and **(D)** Western blot analysis of the expression of MARCO in unstimulated ThioM Φ . **(E)** Real-time PCR analysis of the expression of MMP9 in ThioM Φ . **(F)** MMP9 Western blot. **(G)** Detection of MMP9 activity by gelatin zymography. **(H)** Real-time PCR analysis of the expression of plasminogen activator, urokinase type (uPA). **(I)** Casein zymography of uPA activity in tissue culture supernatants (SN) or cell lysates. Results were confirmed in three independent experiments.

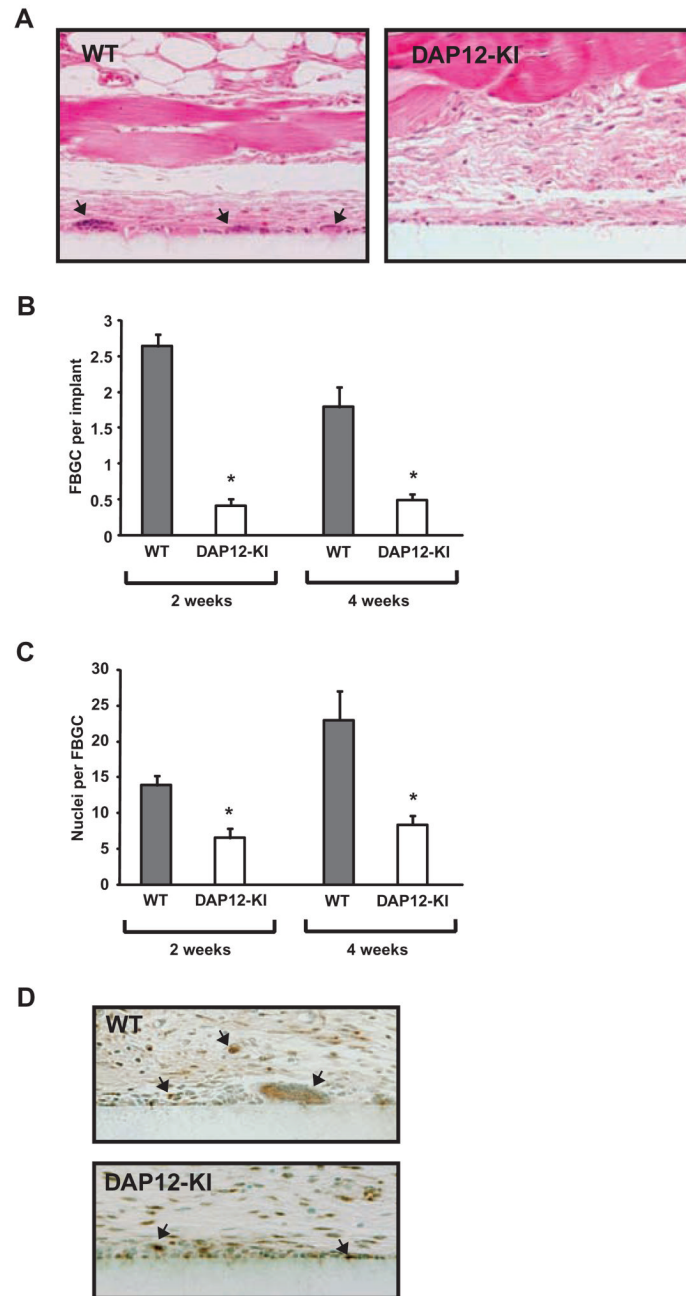


Fig. 10. DAP12 signaling is required for the formation of foreign body giant cells (FBGCs) in vivo. Millipore filters were implanted subcutaneously in WT and DAP12-KI for 2 and 4 weeks. **(A)** Representative images of sections stained with hematoxylin and eosin. Arrows indicate the presence of FBGCs. **(B)** Quantitation of the number of FBGCs per high-power field (200 μm of surface) implant. Shown are means \pm SEM (2 weeks, five animals; 4 weeks, six animals), $*P \leq 0.005$ (compared to WT, Student's *t* test, two-tailed). **(C)** Quantitation of the number of nuclei per giant cell. Shown are means \pm SEM (2 weeks, five animals; 4 weeks, six animals), $P \leq 0.005$ (compared to WT, Student's *t* test, two-tailed). **(D)** Representative images of sections stained with antibodies against MAC3. The presence of mononuclear and multinucleated

macrophages is evident in DAP12-KI sections (arrows); staining was detected with HRP-conjugated secondary antibodies and nuclei were counterstained with methyl green.